

Preparation and Size Determination of Soluble Cross-Linked Macromolecule of Polyurethane

Fangxing Li,^{*,†,‡} Zunfen Lu,[‡] Haitao Qian,[‡] Jiaming Rui,[‡] Shengnan Chen,[‡] Ping Jiang,[‡] Yingli An,[†] and Huaifeng Mi[†]

State Key Lab of Functional Polymer Materials for Adsorption and Separation, Tianjin 300071, P.R.C. and Department of Chemistry, Nankai University, Tianjin 300071, P.R.C

Received May 8, 2003; Revised Manuscript Received November 23, 2003

ABSTRACT: We designed a cross-linking polymerization system composed of inter- and intramolecular reactions on the basis of the model of the characteristic random coil morphology of macromolecules in solution. The cross-linking process in the system was controlled, and the soluble intramolecularly cross-linked macromolecule was successfully prepared in concentrated solution. It was found that this kind of macromolecule tends to form molecular clusters in solution by measuring molecular sizes and that the formation and dissociation of molecular clusters is in a nonequilibrium state, which could be a unique solution behavior of cross-linked macromolecules.

Introduction

Macromolecules with cross-linked structures were first synthesized and described in dilute solution by Staudinger and Husemann in 1935.¹ In 1949, Baker prepared this kind of macromolecule by an emulsion polymerization and called them microgels.² Later, microgels were defined as intramolecularly cross-linked macromolecules (ICMs).^{3–5} Some other techniques for the preparation of ICM^{6–9} have been reported too, but dilute solution polymerization^{10–12} and emulsion polymerization^{13–17} are still typical methods. Though these methods are clever techniques for the synthesis of ICM, they fail to control the cross-linking process, the main cause for which is the absence of a competitive reaction with the intermolecular reaction (cross-linking reaction) in the system. In this work, a cross-linking polymerization system composed of a pair of competitive reactions was designed to control the cross-linking process.

Random coil, the basic morphology of a macromolecule in solution, is an important base case on which we designed a cross-linking polymerization system composed of a pair of competitive reactions. The formation of ICM is based on a favorable competition between intramolecular reaction (involving functional groups of a single chain) and intermolecular reaction (between functional groups of different chains). Since the reactivity in intra- and intermolecular reactions is the same, the fraction of intra- vs intermolecular reaction will only depend on the relative probability of encountering another internal functional groups relative to that associated with the intermolecular reaction.

The prepolymer with two kinds of functional groups that could react with each other was first synthesized. Figure 1 shows the intra- and intermolecular reactions.

In Figure 1, a reactive end group on coil surface (shown as *a*) takes part in the intermolecular reaction. If this reaction were not inhibited, the gelation would occur in the system. Another reactive end group inside

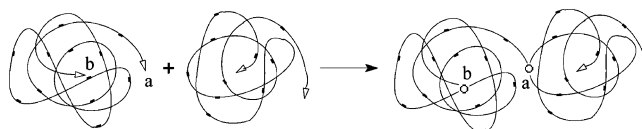


Figure 1. Intra- and intermolecular reactions: rectangle, reactive groups on the macromolecular chain; arrow, reactive end group; ○, cross-linking point.

the coil (shown as *b*) carries out the intramolecular reaction without increasing the molecular weight. If the fraction of the intramolecular reaction is high enough to consume a great amount of functional groups, the concentration of the reactive groups on coil surface will be below the critical level to permit further intermolecular reaction. Thus, the cross-linking process is controlled and soluble ICM is synthesized.¹⁸

ICMs are inclined to form molecular clusters (MCs) in solution, and the formation and dissociation of MCs is in a nonequilibrium state, resulting in the continuous change of the particle size. This is probably caused by the aggregation (entanglement in some literature^{19–22}) of ICMs due to their three-dimensional network. The aggregation is a mechanical interaction, which causes the formation and dissociation of MCs to be in a nonequilibrium state.

Experimental Section

1.1. Materials. Poly(oxytetramethylene) glycol (PTMG; M_n 1684) was prepared in our laboratory.²³ 4,4'-Diphenyl methane diisocyanate (MDI; Wanhua Co., Yantai, PRC), 1,4-butanediol (BD; Plant of chemical reagent, Tianjin, PRC) and dimethylformamide (DMF; Plant of chemical reagent, Tianjin, PRC) were purified by low-pressure distillation prior to use.

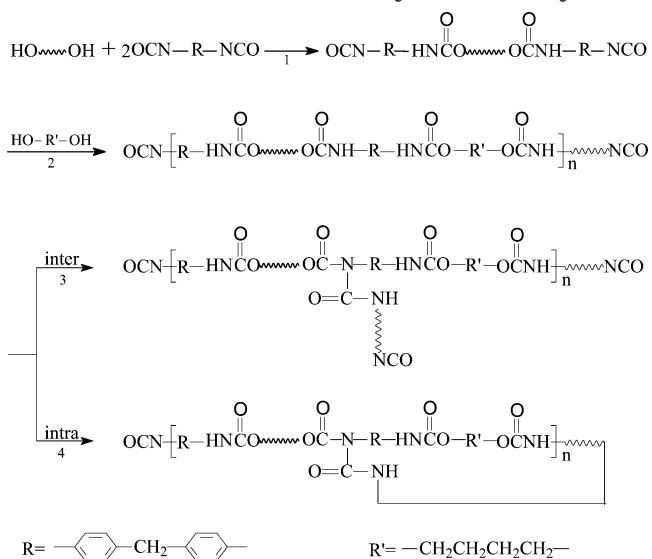
1.2. Polymerization. The polymerization was carried out in a four-neck flask equipped with a stirring bar. Under the protection of dry nitrogen, 12.3204 g of MDI was melted in the dry flask. Then 41.4951 g of PTMG was slowly added dropwise into the flask and maintained at 60 °C for 1 h. The reaction mixture was then cooled to room temperature and 150 mL of DMF and BD (2.2185, 1.5530, and 1.1093 g for the three samples respectively) were added. The mixture was kept at room temperature for 0.5 h, then the temperature was raised to 80 °C, and the reaction was continued for 4 h. Then, the polymer solution was poured into a mold to remove the solvent. After most of the solvent vaporized, the sample was

* To whom correspondence should be addressed. E-mail: lifangxing@nankai.edu.cn.

[†] State Key Lab of Functional Polymer Materials for Adsorption and Separation.

[‡] Nankai University.

Scheme 1. Reactions in the Polymerization System



dried to constant weight at 70°C under vacuum. The PTMG/MDI/BD molar ratios were 1/2/1, 1/2/0.7, and 1/2/0.5, respectively.

1.3. Molecule Size. Photon correlation spectrometer (PCS) was used to determine the polymer molecular size at 25 °C, with a BI-900-AT Correlator, a BI-200-SM Photometer, and an Innova 304 Argon laser. λ was 514.5 nm, the power was 1 w (Coherent Co.), while the practical power was under 200 mW. The solvent was DMF. The dust in solution was removed by ultracentrifugation.²⁴

1.4. Scanning Electron Microscopy. Scanning electron microscopy (SEM) powder samples were prepared by precipitating the polymer solution in distilled water. The precipitates were then dried under vacuum. The images were obtained using a Hitachi S-3500N scanning electron microscope.

1.5. IR Analysis. IR spectra of solid samples were recorded using an AVATAR 360 FT-IR spectrometer.

2. Results and Discussion

2.1. Synthesis of ICMs. 2.1.1 Polymerization Process. The main reactions are shown in Scheme 1.

The oligomer capped with -NCO is formed by reaction 1, and the chain extension step is shown in reaction 2. In this step, reducing the amount of the chain extender leads to the formation of NCO -terminated prepolymers.²⁵ Noted in reaction 2, many -NHCOO- groups exist on the prepolymer chains, and the reaction of NCO with NHCOO results in cross-linking of the prepolymer.²⁶ Reaction 3 occurs between two macromolecules, which is called an intermolecular reaction. Reaction 4 occurs inside a macromolecule, which is called an intramolecular reaction. The two reactions are a pair of competitive reactions. In the early stage of polymerization, the coil is relatively small and a great amount of reactive end groups appear on the coil surface, resulting in a high proportion of the intermolecular reaction. As the polymerization proceeds, the bigger the coil is formed and the more end groups it wraps inside. In the later stage of the polymerization, the intramolecular reaction is favored over the intermolecular reaction, as a result, no gelation occurs in the polymerization system and the soluble cross-linked macromolecule is formed.

Stacked plots of IR spectra of 1684BD-1 and 1684BD-0.5 are shown in Figure 2. The peak at 1731.6 cm^{-1} represents the carbonyl ($\text{C}=\text{O}$) of the $-\text{NHCOO}-$ group. In the IR spectra of 1684BD-1, the shoulder peak at

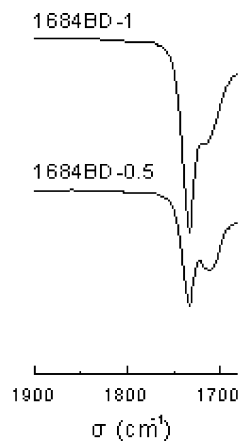


Figure 2. FT-IR spectra of 1684BD-1 and 1684BD-0.5.

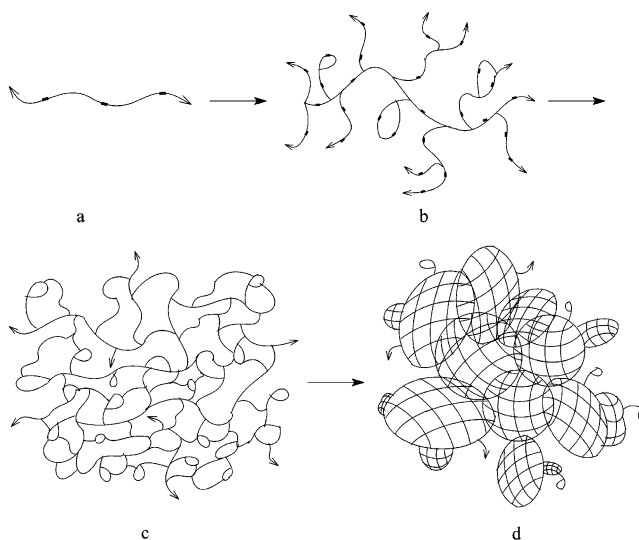


Figure 3. Schematic representation of the chain-growth process.

1714.3 cm^{-1} represents C=O of the $-\text{NCONH}-$ group, whose appearance would be attributed to the inevitability of reactions 3 and 4 in the polymerization system of 1684BD-1. In the IR spectra of 1684BD-0.5, the shoulder peak of C=O of the $-\text{NCONH}-$ group shifts from 1714.3 to 1709.1 cm^{-1} and its intensity increases, which can be ascribed to the formation of more $-\text{NCONH}-$ groups due to the decrease in the amount of the chain extender.

2.1.2. Chain-Growth Process. A chain growth model is shown in Figure 3. A prepolymer (shown as *a*) is formed by reaction 2, and a highly branched macromolecule with a few cyclic structures on the chain (shown as *b*) is formed by reaction 3 and 4 in the early stage of the polymerization due to the relatively small proportion of the intramolecular reaction. A macromolecule with bigger volume and stable network (shown as *c*) is formed by the further reaction. In the later stage of the polymerization, an ICM with huge volume and irregular shape composed of several different sized *c* is obtained, shown as *d*.

The SEM images in Figure 4 show that the superficial morphologies of the samples differ distinctly from each other due to their different degree of cross-linking.

2.1.3. Degree of Cross-Linking. According to the reactions mentioned above, samples 1684BD-1, 1684BD-0.7, and 1684BD-0.5 were synthesized by gradually reducing the amount of the chain extender, where 1, 0.7, and 0.5 are the molar ratio of OH/NCO in reaction

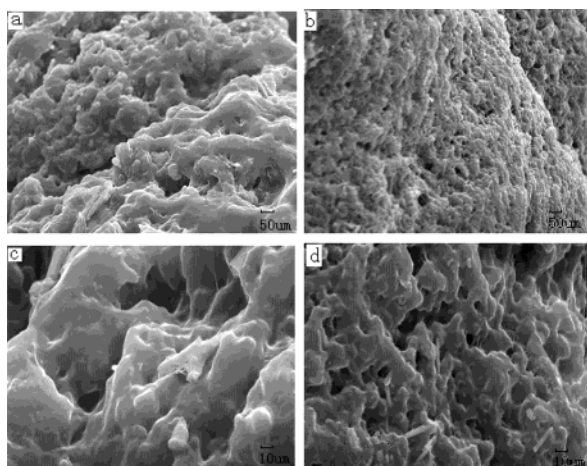


Figure 4. SEM images illustrate the effect of degree of cross-linking on the superficial morphology. (a) 1684BD-1 ($\times 1.0$ k); (b) 1684BD-0.5 ($\times 1.0$ k); (c) 1684BD-1 ($\times 5.0$ k); (d) 1684BD-0.5 ($\times 5.0$ k).

Table 1. Particle Diameters of Sample 1684BD-1 at Different Concentration

no.	I-1 ^b	I-2	I-3	I-4
concn (g/g)	2.05×10^{-3}	2.05×10^{-4}	2.05×10^{-5}	2.05×10^{-6}
particle	1194	606	227	— ^e
diameter (nm)	1073	597	212	—
	1117	658	165	—
	1093	420	192	—
	1075	444	159	—
	1142	418	175	—
AE (nm) ^c	1116	524	188	—
RE (nm) ^d	121	240	68	—

^a In the Tables 2 and 3, RE and AE are processed in the same way. ^b Roman numeral represents the serial number of the sample, and Arabic numeral represents the serial number of the solution. ^c The average number of the six readings. ^d The difference between the maximum and minimum readings. ^e A dash means no reading is obtained at this concentration.

Table 2. Particle Diameters of Sample 1684BD-0.7 at Different Concentration

no.	II-1	II-2	II-3	II-4
concn (g/g)	2.02×10^{-3}	2.02×10^{-4}	2.02×10^{-5}	2.02×10^{-6}
particle	1692	815	1347	775
diameter (nm)	1580	788	1590	829
	1578	806	1559	932
	1528	1277	1915	1218
	1542	1174	1867	889
	1509	1585	1930	918
AE (nm)	1572	1074	1707	927
RE (nm)	183	797	583	443

2 (OH and NCO groups come from the chain extender and the oligomer formed by reaction 1, respectively).

According to reactions 3 and 4 in Scheme 1, the branching reaction will occur when OH/NCO < 1 (molar ratio). The degree of cross-linking (DC) increases with decreasing this ratio, and it can be calculated by eq a.

$$DC = (NCO - OH)/NCO = 1 - OH/NCO \quad (a)$$

For example, the amount of chain extender of 1684BD-0.7 is reduced by 30%, and its degree of cross-linking is just 30%.

2.2. Molecule Sizing. 2.2.1. A Special Phenomenon and the Explanation. The measured results of the molecular sizes of the three samples are shown in Tables 1–3.

It was found in the repetitive measurement that the data of every sample in Tables 1–3 could not be

repeated. Figure 5 shows the plot of particle diameter distribution of no. III-1 at different times. In the four graphs, particle diameter distribution has great variance. In fact, each reading obtained at any time is different. To compare with the solution behavior of the samples, AE and RE are employed to show the average value and the variation range of the particle sizes respectively in Tables 1–3.

As shown in Tables 1–3, the average particle diameter (AE) falls as the concentration decreases, and the particle diameter variation range (RE) decreases as well. It is easy to infer from the results that ICMs tend to form MCs in solution. The unceasing change of the readings indicates the formation and dissociation of MCs is in a nonequilibrium state. The larger the AE is, the larger the MCs will be; the larger the RE is, the formation and dissociation of MCs is farther away from the balance point. The internal structure of macromolecules synthesized in this paper is that of a swollen network, so these macromolecules in solution can entangle with each other and aggregate to form clusters very easily. All clusters in solution change unceasingly, they are disentangling, or several clusters entangle together again. Because of large molecular volume, the entanglement rate is faster than the disentanglement rate, so it is impossible to realize the steady state of the average particle diameter. Just like a cloud in the sky, the particle diameter changes unceasingly, a state that at any time cannot be repeated.

The entanglement between ICMs is greatly different from that between linear macromolecules. Figure 6 shows the entanglement of these two kinds of the macromolecules, respectively. Two linear macromolecules in an extended stretched-out phase (shown as *e* and *f*) might entangle with each other like two snakes (shown as *g*). But this probability is virtually zero, because the linear macromolecules could only exist as random coils instead of expanded lines in solution. Two linear macromolecular coils are shown as *m* and *n* respectively. Two parallel segments (shown as *L*₁ and *L*₂) in *m* constitute an “open mouth”. When a “tongue” composed of some segments penetrates into the mouth, it cannot be bitten tightly due to the very loose structure of the linear macromolecular coil. In other words, the “mouth” does not have a strong muscle (just like a clamp without a spring) and cannot produce a strong mechanical effect. But this is not the case for ICMs. ICMs (shown as *p* and *q* in Figure 6) contain holes on the surface due to their network structure, and the holes are just like mouths with a strong muscle. A “tongue” may be produced on the surface of *q* and enter the hole of *p* to be bitten tightly. Thus, the mechanical aggregation effects together with the van der Waals’ force²⁷ contributes to form MCs in solution in this paper. Because of the irregular shape of ICMs (shown as *d* in Figure 3), the collision sites and mechanical interactions will be greatly different during the repeated collisions, leading to the obviously different mechanical aggregation effects, which cannot be balanced by the dissociation effects produced by the solvent. Therefore, the formation and dissociation of MCs is in a nonequilibrium state, leading to the unceasing change of the readings.

Though the shapes of linear, branched, comb, star, and cyclic macromolecules are obviously different, they all exhibit a planar zigzag structure when fully stretched out, but this is not the case for the ICM. Therefore, we

Table 3. Particle Diameters of Sample 1684BD-0.5 at Different Concentration

no. concn (g/g)	III-1 2.09×10^{-3}	III-2 2.09×10^{-4}	III-3 2.09×10^{-5}	III-4 2.09×10^{-6}	III-5 1.05×10^{-6}
Part 1					
particle diameter (nm)	1345	679	785	324	260
	1182	743	792	293	258
	1353	822	772	311	253
	1647	700	799	296	243
	1315	732	782	281	244
	1267	669	802	284	245
AE (nm)	1352	724	789	289	251
RE (nm)	465	143	30	43	17
Part 2					
particle diameter (nm)	823	678	657	779	— ^a
	717	675	658	784	—
	756	659	663	794	—
	690	647	671	803	—
	686	652	683	810	—
	684	661	665	808	—
AE (nm)	726	662	666	796	—
RE (nm)	139	31	26	29	—

^a A dash means that the particle size is not determined at this concentration.

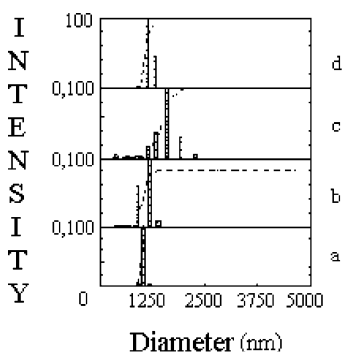


Figure 5. Particle diameter distribution obtained by CONTIN analysis of no. III-1 at different times: (a) 1182 nm; (b) 1647 nm; (c) 1353 nm; (d) 1315 nm.

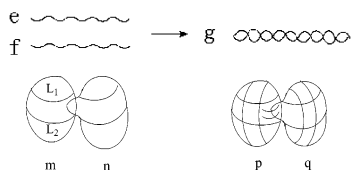


Figure 6. Entanglement of macromolecules.

have to attribute this special solution behavior to the network structure of ICM.

2.2.2 Influence of the Concentration and Amount of Chain Extender on AE and RE. According to eq a, the degree of cross-linking of 1684BD-1 is zero, but the IR spectra reflect that the macromolecules of 1684BD-1 also have the cross-linked structure with low cross-link density. In Table 1, AE decreases monotonically with decreasing concentration. No reading is obtained at the concentration of no. I-4, probably because the macromolecule is relatively small.

Table 2 shows the solution behavior of 1684BD-0.7. The larger AE of 1684BD-0.7 compared with 1684BD-1 can be attributed to its higher cross-link density, which provides a higher MCs-forming ability. The larger RE indicates that the formation and disassociation of MCs of 1684BD-0.7 is farther away from the balance point. With decreasing concentration, AE decreases at first, and then increases, and finally decreases again. Therefore, we infer that two effects take on certain roles and cast the other in corresponding counter roles in affecting the particle size. One is the dissociation effect that

decreases the particle size, and the other is the network swelling effect that increases the ability of aggregation of ICMs. If the former is predominant, the particle diameter will decrease. If the latter is favored, the particle diameter will increase. Among the six readings of no. II-4 only one is much higher than the others, indicating that the single molecular state has been achieved, accompanying with occasional appearance of MCs.²⁸ And we infer the single molecular diameter might be about 800 nm, not 927 nm.

There are two parts in Table 3. Part 1 shows the results obtained as soon as the sample was completely dissolved (it took 3 days to dissolve); part 2 shows the results obtained 30 days after the sample was completely dissolved.

In this section, part 1 in Table 3 is discussed. 1684BD-0.5 has a higher cross-link density than 1684BD-0.7, but it has a smaller AE compared with 1684BD-0.7, as shown in no. III-1. This reflects that the surface of ICM tends to be smooth with increasing network density, resulting in the decrease in the MC-forming ability.²⁹ With falling the concentration, AE of 1684BD-0.5 decreases sharply at first, and then increases a little, and then decreases sharply again, and finally almost remains constant. It is indicated that the interaction of dissociation effect with network swelling effect is causing the change of particle size. The constant AE of no. III-4 and no. III-5 indicates that AE of no. III-4 would probably be the single molecular size.²⁸

2.2.3. Influence of Time on Particle Diameter. Segmented polyurethanes (SPU) are multiblock copolymers with a distribution of hard- and soft-segment blocks. The hard and soft phases tend to segregate due to their immiscibility, and produce a phase-separated morphology of hard-segment-rich and soft-segment-rich phases that are connected through urethane linkages. The thermodynamic driving force for minimizing the total free energy of the system results in preferential surface segregation of the lower surface energy constituent (soft-segment block) of the polymer.^{30,31} ICM in this work is also composed of the similar hard and soft segments, and similar phase segregation also occurs in ICM and contributes to the decrease of particle size. On one hand, when the hard segments are covered by the soft-segment-rich phases, MCs-forming ability will be decreased. On the other hand, the association of hard

segments acting as physical cross-links leads to a shrunken volume and greater surface smoothness of ICM and then decreases the MC-forming ability. Sample 1684BD-0.5 has almost the same AE in different concentration solutions 30 days after it was completely dissolved, as shown in part 2 of Table 3. It is indicated that the particles in solution exist almost as single molecules. The relatively larger AE in no. III-1 may be caused by the retained few MCs in solution, and the relatively larger AE in no. III-4 may be caused by the more substantially swollen ICMs.

2.2.4. Judgment of the Single Molecular Size.

Judgment of single molecular size is complicated because ICMs tend to swell and aggregate in solution.

Sample 1684BD-1 exists as MCs in solution nos. I-1 to I-3, and the experimental results of solution no. I-4 are not obtained, so we cannot get a single molecular size of this sample.

The sample 1684BD-0.7 swells substantially in a short period of time in solution due to its intermediate degree of cross-linking, so its swollen single molecular size is obtained in no. II-4.

The MCs of the sample 1684BD-0.5 disassociate substantially in no. III-4 in part 1 of Table 3, so we can get its single molecular size. But this sample cannot swell substantially in a short period, so we can see that the single molecular size rises as time goes on. The size of not fully swollen single molecule is shown in no. III-4 in part I of Table 3, and that of fully swollen one is obtained 30 days after the sample was resolved, as shown in no. III-4 in part 2 of Table 3.

2.3. Potential Energy of Network. During the development of cross-linked structure, as shown in Figure 3, coils (*b* or *c*) join each other by covalent bonds disorderedly. Therefore, they have not enough time to settle to their lowest potential energy state before they are joined to the network in at least two points encompassing the cross-link site and become "fixed". Therefore, potential energy is stored in the network.

During the volatilization of solvent, the potential energy cannot be released due to the extrusion among the ICMs. When the sample is resolved in dilute solution, coils (*b* or *c*) tend to settle to their lowest potential energy state. And it will take a long period of time for the ICMs with high degree of cross-linking to reach the lowest energy state of the network. The tendency of ICMs to form MCs and the unbalance of formation and dissociation of MCs are both a reflection of the release of the potential energy.

Conclusion

1. In the cross-linking polymerization system consisting of intra- and intermolecular reactions, the cross-linking process can be controlled, so soluble macromolecules with cross-linked structure is synthesized.

2. ICMs tend to form MCs, and the formation and dissociation of MCs is in a nonequilibrium state.

3. The main reason for ICMs to form MCs is due to the three-dimensional network structure of ICMs.

References and Notes

- (1) Staudinger, H.; Husemann, E. *Ber. Dtsch. Chem. Ges.* **1935**, *68*, 1618–1634.
- (2) Baker, W. O. *Ind. Eng. Chem.* **1949**, *41*, 511–520.
- (3) Funke, W.; Bauer, H.; Joos, B.; Kaczun, J.; Kleiner, B.; Leobelt, U.; Okay, O. *Polym. Int.* **1993**, *30*, 519–523.
- (4) Abrol, S.; Solomon, D. H. *Polymer* **1999**, *40*, 6583–6589.
- (5) Abrol, S.; Caulfield, M. J.; Qiao, G. G.; Solomon, D. H. *Polymer* **2001**, *42*, 5987–5991.
- (6) Kim, K. S.; Cho, H. S.; Shin, J. S. *Polym. J.* **1995**, *27*, 508–514.
- (7) Kim, K. S.; Cho, H. S.; Kim, Y. J. *Polym. J.* **1993**, *25*, 847–851.
- (8) Downey, J. S.; McIsaac, G.; Frank, R. S.; Stöver, H. D. H. *Macromolecules* **2001**, *34*, 4534–4541.
- (9) Schmitz, K. S.; Wang, B.; Kokufuta, E. *Macromolecules* **2001**, *34*, 8370–8377.
- (10) Okay, O.; Durmaz, S.; Erman, B. *Macromolecules* **2000**, *33*, 4822–4827.
- (11) Rangelov, S.; Brown, W. *Polymer* **2000**, *41*, 4825–4830.
- (12) Szuromi, E.; Berka, M.; Borbely, J. *Macromolecules* **2000**, *33*, 3993–3998.
- (13) Miyata, M.; Funke, W. *Makromol. Chem.* **1983**, *184*, 755–762.
- (14) Funke, W.; Walther, K. *Polym. J.* **1985**, *17*, 179–187.
- (15) Zhao, Y.; Zhang, G. Z.; Wu, C. *Macromolecules* **2001**, *34*, 7804–7808.
- (16) Lindenblatt, G.; Scharlt, W.; Pakula, T.; Schmidt, M. *Macromolecules* **2000**, *33*, 9340–9347.
- (17) Fernández-Nieves, A.; Fernández-Barbero, A.; Vincent, B.; de las Nieves, F. J. *Macromolecules* **2000**, *33*, 2114–2118.
- (18) Frank, R. S.; Downey, J. S.; Yu, K.; Stöver, H. D. H. *Macromolecules* **2002**, *35*, 2728–2735.
- (19) Terzis, A.; Theodorou, D. N.; Stroeks, A. *Macromolecules* **2000**, *33*, 1385–1396.
- (20) Terzis, A.; Theodorou, D. N.; Stroeks, A. *Macromolecules* **2000**, *33*, 1397–1410.
- (21) Terzis, A.; Theodorou, D. N.; Stroeks, A. *Macromolecules* **2002**, *35*, 508–521.
- (22) Semenov, A. N. *Macromolecules* **2002**, *35*, 4821–4837.
- (23) Li, F. X.; Wang, H. J.; Li, C. G.; Ma, K. Q. *J. Polym. Sci., Part A: Polym. Chem.* **1994**, *32*, 1939–1947.
- (24) Zuo, J. In: *Principles and Applications of Laser Light Scattering in Polymer Science*; Han, J. X., Ed.; Press of Science and Technology: Henan, PRC, 1994; p 65.
- (25) Li, F. X.; Zuo, J.; Dong, L. M.; Wang, H. J.; Luo, J. Z.; et al. *Eur. Polym. J.* **1998**, *34*, 59–66.
- (26) Lyman, D. J. The Chemistry of the Diisocyanate-Diol reaction. In *Step-Growth Polymerizations*, 2nd ed.; Solomon, D. H., Ed.; Marcel Dekker Inc.: New York, 1972; p 98.
- (27) Yoshida, E.; Kunugi, S. *Macromolecules* **2002**, *35*, 6665–6669.
- (28) Li, F. X.; Zuo, J.; Song, D. H.; Li, Y. T.; Ding, L. H.; An, Y. L.; Wei, P.; Ma, J. B.; He, B. L. *Eur. Polym. J.* **2001**, *37*, 193–199.
- (29) Senff, H.; Richtering, W. *Colloid Polym. Sci.* **2000**, *278*, 830–840.
- (30) Garrett, J. T.; Siedlecki, C. A.; Runt, J. *Macromolecules* **2001**, *34*, 7066–7070.
- (31) Hearn, M. J.; Ratner, B. D.; Briggs, D. *Macromolecules* **1988**, *21*, 2950–2959.

MA034593K